Comparison between Navier-Stokes and DSMC Calculations for Low Reynolds Number Slip Flow Past a Confined Microsphere

S.K. Stefanov[*], R.W. Barber[**], M. Ota[***] and D.R. Emerson[**]

[*]*Institute of Mechanics, BASci., Acad. G. Bonchev Str., Bl. 4, Sofia 1113, Bulgaria*
[**]*Centre for Microfluidics, CCLRC Daresbury Laboratory, Daresbury, Warrington, WA4 4AD, UK*
[***]*Tokyo Metropolitan University, Dept. Mech. Eng., 1-1 Minami-Ohsawa, Hachioji-shi, Tokyo 192-0397, Japan*

Abstract. In the present investigation, slip-continuum and molecular (DSMC) flow models have been used to compare the drag coefficient on a confined microsphere over a range of Knudsen numbers between 0.01 and 0.4. The simulations consider a fixed Reynolds number (Re=0.125) and a range of blockage ratios from 2.0 up to 13.0. Two separate problem formulations have been studied; the first considers flow past a confined sphere moving with a constant velocity along the central axis of the pipe while the second considers Poiseuille flow past a stationary confined sphere. Finally, their combination - the case of a confined sphere moving within the carrier Poiseuille flow is investigated using the DSMC method.

INTRODUCTION

The emergence of Micro-Electro-Mechanical-Systems (MEMS) as a key enabling technology has led to the development of an increasing number of gas-phase microfluidic systems. Potential applications are numerous and include miniaturised heat exchangers, portable gas chromatography systems, miniaturised gas sensors and novel high-throughput gas flow cytometers. However, one of the most important issues influencing MEMS research is the growing realisation that gas-phase microflows are dominated by non-continuum or rarefaction effects.

Previous numerical studies by the authors have investigated the important problem of low Reynolds number slip flow past a confined microsphere within a circular pipe [1,2]. The simulations were conducted using two different numerical approaches based upon continuum (Navier-Stokes) [1] and molecular (DSMC) [2] model descriptions. The studies have resulted in a number of fundamental questions regarding the application of both conventional (continuum) and molecular (DSMC) models for gas microflows. One such question concerns the upper limit of Knudsen number for which a continuum slip-boundary solution might be valid. Another is whether the DSMC method is able to cover a sufficiently wide range of Knudsen numbers so that continuum and molecular data can be compared.

In the present investigation, slip-continuum and molecular models have been used to compare the drag coefficient on a confined microsphere over a range of Knudsen numbers between 0.01 and 0.4. The simulations consider a fixed Reynolds number (Re=0.125) and a range of blockage ratios, B = (pipe diameter)/(microsphere diameter) from B=2.0 up to B=13.0. Two separate problem formulations have been studied; the first considers flow past a confined sphere moving with a constant velocity along the central axis of the pipe while the second considers Poiseuille flow past a stationary confined sphere. The continuum model employs a tangential slip-velocity boundary condition and assumes that compressibility effects can be neglected while the molecular simulations are conducted using a standard DSMC method. The DSMC approach allows non-equilibrium and rarefaction effects to be captured over a wide range of Knudsen numbers but has the disadvantage of requiring extremely large numbers of particles at low Knudsen numbers, making the technique prohibitively expensive in terms of computational cost. The reason is that the macroscopic gradients and bulk velocity in micro-flows of practical interest are usually small and the statistical error of the DSMC calculations is comparable to the magnitude of the macroscopic flow characteristics.

CP762, *Rarefied Gas Dynamics: 24th International Symposium,* edited by M. Capitelli

Report Documentation Page

Form Approved
OMB No. 0704-0188

1. REPORT DATE	2. REPORT TYPE	3. DATES COVERED
13 JUL 2005	**N/A**	**-**

4. TITLE AND SUBTITLE	5a. CONTRACT NUMBER
Comparison between Navier-Stokes and DSMC Calculations for Low Reynolds Number Slip Flow Past a Confined Microsphere	5b. GRANT NUMBER
	5c. PROGRAM ELEMENT NUMBER
6. AUTHOR(S)	5d. PROJECT NUMBER
	5e. TASK NUMBER
	5f. WORK UNIT NUMBER
7. PERFORMING ORGANIZATION NAME(S) AND ADDRESS(ES) **Institute of Mechanics, BASci., Acad. G. Bonchev Str., Bl. 4, Sofia 1113, Bulgaria**	8. PERFORMING ORGANIZATION REPORT NUMBER
9. SPONSORING/MONITORING AGENCY NAME(S) AND ADDRESS(ES)	10. SPONSOR/MONITOR'S ACRONYM(S)
	11. SPONSOR/MONITOR'S REPORT NUMBER(S)

12. DISTRIBUTION/AVAILABILITY STATEMENT
Approved for public release, distribution unlimited

13. SUPPLEMENTARY NOTES
See also ADM001792, International Symposium on Rarefied Gas Dynamics (24th) Held in Monopoli (Bari), Italy on 10-16 July 2004.

14. ABSTRACT

15. SUBJECT TERMS

16. SECURITY CLASSIFICATION OF:			17. LIMITATION OF ABSTRACT	18. NUMBER OF PAGES	19a. NAME OF RESPONSIBLE PERSON
a. REPORT **unclassified**	b. ABSTRACT **unclassified**	c. THIS PAGE **unclassified**	**UU**	**6**	

The DSMC calculations have shown that these difficulties can be overcome, under certain conditions, by using a simple data filter for computing the averaged flow fields. It should be noted that a promising alternative approach is the information preservation method proposed by Fan and Shen [3]. In the present paper, the DSMC approach has been used to simulate flows down to a Knudsen number, Kn = (mean free path)/(sphere diameter) of 0.01 for a blockage ratio of B=2.0, Kn=0.02 for B=5.0, and Kn=0.04 for B=13.0 (approaching the case of an unconfined sphere). For this last case, the drag force has also been compared against the analytical expression for the drag on an unconfined sphere presented by Beresnev *et al*. [4]. In this case, the continuum slip-flow calculations overpredict the drag coefficient at all Knudsen numbers but converge to the Beresnev solution as Kn tends to zero. The DSMC results show good agreement with Beresnev *et al*.'s analytical solution for $Kn > 0.04$. In the case of a confined sphere, the continuum model predicts a larger drag coefficient than the DSMC method when Kn is larger than some critical value that depends on the blockage ratio. However, at very small Knudsen numbers, the DSMC simulations predict a larger drag coefficient than the continuum slip model. This interesting result may be explained by the effects of gas compression in front of the microsphere and rarefaction behind it.

Finally, we report some preliminary DSMC results concerning a more realistic case of flow past a confined sphere moving within the carrier fluid along the central axis of the pipe. In other words, we have generalized the problem and considered the combination of the two limiting formulations mentioned above. The combined formulation makes it possible to estimate the relative motion between the sphere and the bulk flow.

PROBLEM FORMULATION

We consider a monatomic gas flow past a confined microsphere with diameter, D, in a circular pipe with diameter, H ($H > D$). The flow is simulated using an axially-symmetric computational domain with a finite length, L. The computational domain and the imposed local cylindrical coordinate system (x,r) are shown in Fig. 1. Initially, the pipe is filled with gas of density, $\rho_0=mn_0$ (m is the mass of the gas molecules and n_0 is the number density) and temperature, T_0. The pipe wall and the inlet/outlet gas fluxes are assumed to have the same temperature, T_0. Diffuse reflection, or a corresponding slip-velocity boundary condition, is assumed on both the pipe and particle surfaces.

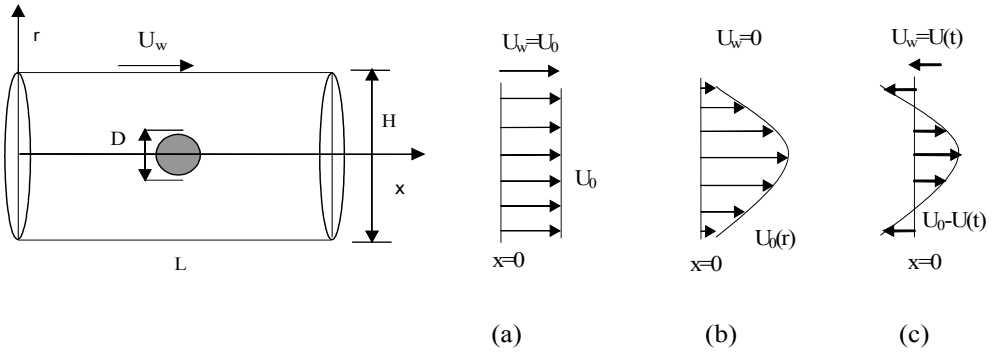

FIGURE 1. Local computational domain around the sphere. Inflow velocity profile U_0 and boundary velocity U_w for: case (a), a confined sphere moving with a constant velocity along the central axis; case (b), Poiseuille flow past a stationary confined sphere; case (c), a confined sphere moving with velocity $U(t)$ in the Poiseuille flow.

Under these general conditions we have studied three flow regimes. The first case concerns a confined sphere moving with a constant velocity U_0 along the central axis (as shown in Fig. 1(a)). In the local coordinate system this means that the sphere is at rest while the pipe wall is moving with velocity $U_w=U_0$. The inflow at x=0 has a uniform velocity profile, U_0. At the outlet, the axial gradients of the velocity components are assumed to be zero.

The second case concerns Poiseuille flow past a stationary confined sphere (Fig. 1(b)). In the local coordinate system, the wall velocity U_w=0. At the inflow boundary (x=0), a fully-developed slip-velocity profile [1] is prescribed parallel to the longitudinal axis of the pipe:

$$U_0(r) = 2\overline{U}\left(1-\frac{4r^2}{H^2}+4\frac{2-\sigma}{\sigma}\frac{Kn}{H/D}\right)\Big/\left(1+8\frac{2-\sigma}{\sigma}\frac{Kn}{H/D}\right) \qquad (1)$$

where $\overline{U}$ is the mean velocity in the pipe and σ is the tangential momentum accommodation coefficient (σ = 1 for diffuse reflection). At the outlet, the axial gradients of the velocity components were assumed to be zero.

The third case (Fig. 1(c)) is a combination of the first two and describes the microsphere motion along the central axis. The motion is induced by the drag of the carrier Poiseuille flow. The instantaneous velocity of the sphere $U(t)$ is computed from the equation:

$$m_p \frac{dU(t)}{dt} = F_D(t), \tag{2}$$

where m_p is mass of the sphere and $F_D(t)$ is the instantaneous drag force acting on the sphere. For simplicity, in Eq. (2) we have neglected Brownian motion and assumed there are no external forces on the sphere. The initial condition is $U(0)=0$. In the imposed coordinate system, the inflow condition, Eq. (1), at $x=0$ is modified to give

$$U_0'(t) = U_0 - U(t). \tag{3}$$

The wall velocity thus becomes $U_w = -U(t)$. For clarity in the computational algorithm used for case (c), it should be noted that the longitudinal component of the velocity field, $U(t,x,r)$, computed in the local coordinate system, was also modified each time step:

$$U(t+\Delta t, x, r) = U(t, x, r) - \frac{dU(t)}{dt}\Delta t. \tag{4}$$

Numerical simulations were used to assess the drag experienced by a confined sphere exposed to low Reynolds number flow. In case (a), the Reynolds number, *Re*, was defined using the constant velocity, U_0, and the sphere radius, $a=D/2$, as the velocity and length scales:

$$Re = \frac{\rho a U_0}{\mu}, \tag{5}$$

where μ is the viscosity of the gas, whilst in cases (b) and (c), *Re* was defined using the mean velocity in the pipe, $\overline{U}$, instead of U_0. The second parameter, the Knudsen number, $Kn=\lambda/D$, determines the degree of rarefaction of the gas. The mean free path of molecules, λ, was defined for an ideal gas modeled as rigid spheres with diameter d (Eq. (9)). Blockage effects were studied by varying the ratio between the diameter of the confining pipe, H, and the diameter of the sphere, D.

COMPUTATIONAL CONSIDERATIONS

For flow cases (a) and (b), slip-continuum and molecular models have been used to compare the drag coefficient on a confined microsphere over a range of Knudsen numbers between 0.01 and 0.4. All simulations consider a fixed Reynolds number ($Re=0.125$) and a range of blockage ratios from $B=2.0$ up to $B=13.0$ (for the molecular model) and from $B=2.0$ up to $B=40.0$ (for the slip-continuum approach). The continuum model assumes that compressibility effects can be neglected and employs a tangential slip-velocity boundary condition at the pipe wall and surface of the microsphere:

$$u_t = \frac{2-\sigma}{\sigma}\frac{KnD}{\mu}\tau_t, \tag{6}$$

where τ_t is the shear stress at the surface. The governing hydrodynamic equations [1] were solved using a two-dimensional finite-volume Navier-Stokes solver developed by the Computational Engineering Group at CCLRC Daresbury Laboratory.

The molecular simulations were conducted in a two-dimensional cylindrical domain $(x,r) \in (0,L)\times(0,H/2)$ using standard DSMC procedures for simulation of flows with axial symmetry [5]. The computational domain was covered by a uniform rectangular basic grid with $N_x \times N_r$ cells. For the most difficult computational case ($Kn=0.04$, $B=13.0$), a pipe domain with dimensions $(L,R)=(64\times20)$ μm was employed and the radius of the spherical particle was taken as $R_p=1.55$ μm. The total number of simulated molecules in the pipe volume was approximately 20×10^6. In this case, the computational domain was covered by a grid with 2400×800 basic cells. The basic cells near the surface of the sphere were subdivided dynamically into subcells in order to meet the spatial resolution requirements of the method. Flow field sampling was conducted on a coarser grid with larger cells containing 20×20 basic cells. This multilevel grid scheme allowed the calculation of the molecular processes correctly on an adaptive fine grid and

at the same time provided a meaningful sample size for the macroscopic variables. In addition, a simple filtering procedure was applied along with standard time averaging of the accumulated flow field data. For all cases, the computed temperature was T_0=288 K. The smallest time step used for computing the near-continuum cases was Δt=1.0×10^{-10} s. The force acting on the sphere was determined from the rates of delivery and removal of momentum by incident and reflected molecules from the particle surface within a time interval, Δt_s:

$$< F_x >= \frac{1}{\Delta t_s} \sum m\left(V_x^{(+)} - V_x^{(-)}\right). \tag{7}$$

In case (c), the instantaneous value of the drag force was taken to be $F_D(t) = <F_x(t)>$ estimated over a small macroscopic scale time interval $\Delta t_s=(t-t_s)=(1\sim5)10^2\Delta t$. In cases (a) and (b), the drag force was averaged over a large time interval, $\Delta t_s=10^5\Delta t$, after reaching the steady-state flow conditions.

NUMERICAL RESULTS

The slip-continuum Navier-Stokes (NS) and molecular model (DSMC) results were compared for two separate flow problems (case (a) and case (b)). The Knudsen number, *Kn*, and the blockage ratio, *B*, were varied while the Reynolds number was fixed at a small value, *Re*=0.125. Since the slip-continuum model assumes a constant density, the variation of the Knudsen number does not affect the Reynolds number and, consequently, for fixed *Re*, there is no correlation between gas density and flow velocity when changing *Kn*. This is not the case with the molecular model. All DSMC results were obtained in dimensional form using the "hard sphere" model with a molecular mass of 4.815×10^{-26} kg and a molecular diameter of 3.7×10^{-10} m. Under these conditions, the mean free path variation for a gas in equilibrium depends only on the gas density. Thus, to keep *Re* constant, when changing *Kn*, the product (ρU) must be also kept constant. It can easily be shown that the following relation between *Re*, *Kn* and Mach number, *Ma*, is valid for a monatomic hard sphere gas:

$$Re = \sqrt{\frac{32}{15\pi}}\,\frac{Ma}{Kn}, \tag{8}$$

where the Mach number and the Chapman-Enskog first approximation for viscosity and mean free path are

$$Ma = \frac{U}{\sqrt{(5/3)kT_0/m}}, \quad \mu = \frac{5}{16}\lambda\sqrt{\frac{2\pi kT_0}{m}}, \quad \lambda = (\sqrt{2}\pi d^2 n_0)^{-1}. \tag{9}$$

Equation (8) indicates that to keep *Re* constant while changing *Kn*, necessitates changing the Mach number, *Ma*.

Case (a): Confined Sphere Moving with a Constant Velocity

For case (a), the slip-continuum Navier-Stokes (NS) calculations were performed for a range of Knudsen numbers from *Kn*=0.0 (continuum flow regime) to *Kn*=0.4 and a range of blockage ratios from *H*/*D*=2 to *H*/*D*=40. The latter can be considered as approaching the case of an unconfined sphere. The molecular (DSMC) approach was used to simulate flows down to a Knudsen number, *Kn*=0.01 for a blockage ratio of *B*=2.0, *Kn*=0.02 for *B*=5.0, and *Kn*=0.04 for *B*=13.0 (approaching the case of an unconfined sphere). We compare the normalized total drag coefficient on the microsphere, $C_D Re/12$ [1] versus the Knudsen number for three separate blockage ratios, *B*=2.0, *B*=5.0 and *B*=13.0 (DSMC) and *B*=40.0 (NS). For the largest value of *B*, the normalized drag coefficient was also compared against the analytical formula presented by Beresnev *et al*. [4], which is in good agreement with other theoretical and numerical results (see for example [6,7]). For complete diffusive reflection on the surface of the sphere, the normalized analytical drag coefficient [4] can be written as follows:

$$\frac{C_D\,\mathrm{Re}}{12} = \frac{8+\pi}{18}\left[\frac{1}{Kn+0.619}\left(1+\frac{0.310Kn}{Kn^2+1.152Kn+0.785}\right)\right]. \tag{10}$$

The results of the comparison are shown in Fig. 2(a). The DSMC calculations were extended up to *Kn*=10.0. For *B*>>1 (approaching the case of an unconfined sphere) the DSMC results were in good agreement with Beresnev's formula (10). An exception is the data point at *Kn*=0.04 where a meaningful sample size of DSMC data could not be reached. The reason for the observed difference at large *Kn* is the formation of a shock wave when the bulk velocity

exceeds the sonic speed. In the case of an unconfined sphere, the continuum slip-flow calculations overpredict the drag coefficient at all Knudsen numbers but converge to the Beresnev solution as *Kn* tends to zero. In the case of a confined sphere (B=5.0 and B=2.0), the continuum model predicts a larger drag coefficient than the DSMC method when *Kn* is larger than some critical value that depends on the blockage ratio. However, at very small Knudsen numbers, the DSMC simulations predict a larger drag coefficient than the continuum-slip model. This interesting result may be explained by the effects (observed in the DSMC data, Fig. 2(b)) of gas compression in front of the microsphere and rarefaction behind it.

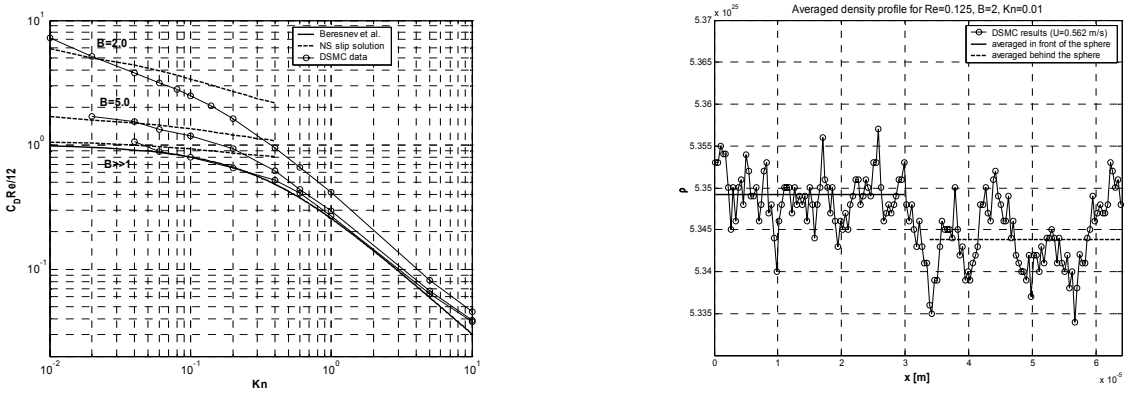

(a) (b)

FIGURE 2. (a) Normalized drag coefficient versus Knudsen number: slip-continuum model (dashed lines); DSMC data (circles). For B>>1 both slip-continuum and DSMC results are compared with the analytical formula, Eq. (10) (solid line); **(b)** Density distribution along the x-axis: DSMC data (circles), averaged density in front of the sphere (solid line), averaged density behind the sphere (dashed line).

Case (b): Gas Flow Past a Stationary Confined Sphere

The normalized drag coefficient obtained for Poiseuille flow past a stationary confined sphere (Fig. 1(b)) is shown in Fig. 3(a). The Knudsen number in the DSMC simulations ranged from 0.01 to 0.6 while the slip-continuum model calculations were performed over the ranges shown in Fig. 3(a). Two aspect ratios, B=2.0 and B=5.0, were considered. The results for B=2.0, case (b) (solid lines), are given together with the corresponding results for case (a) (dash-dot lines). Again, as in case (a), the DSMC computed normalized drag coefficient is larger than the corresponding slip-continuum model at small Knudsen numbers, and less than the continuum approach at large Knudsen numbers. An interesting result observed in the DSMC computed drag coefficient is the larger slope of the curve in case (b) compared to case (a). In contrast, the slope of the slip-continuum results is almost the same in both cases. This difference is demonstrated in Fig. 3(b) which shows the dependence of the dimensional drag force on the Knudsen number for Re=0.125 and B=2.0. It can be seen that the different flow gradients around the sphere have the opposite effect on the drag force variation. In case (a), the drag is approximately proportional to *Kn* while in case (b), the drag is inversely proportional to *Kn*.

Case (c): Confined Sphere Moving with Velocity $U(t)$ in the Carrier Poiseuille Flow

Figure 4(a) illustrates the time evolution of the particle velocity in the pipe under the action of the carrier Poiseuille flow for case (c). The results were obtained for Kn=0.1 using the DSMC method. From Fig. 4(a) one can conclude that the blockage ratio, B, strongly affects the particle velocity. The particle velocity was computed at each time step from Eq. (2), where the mass, m_p, was taken for a sphere with density 1800 kg/m^3. The drag force (Eq. (7)) oscillations (circles) are illustrated in Fig. 4(b) for B=5.0. When the filtered mean drag (thick solid line) tends to zero, the corresponding velocity asymptotically reaches its constant value.

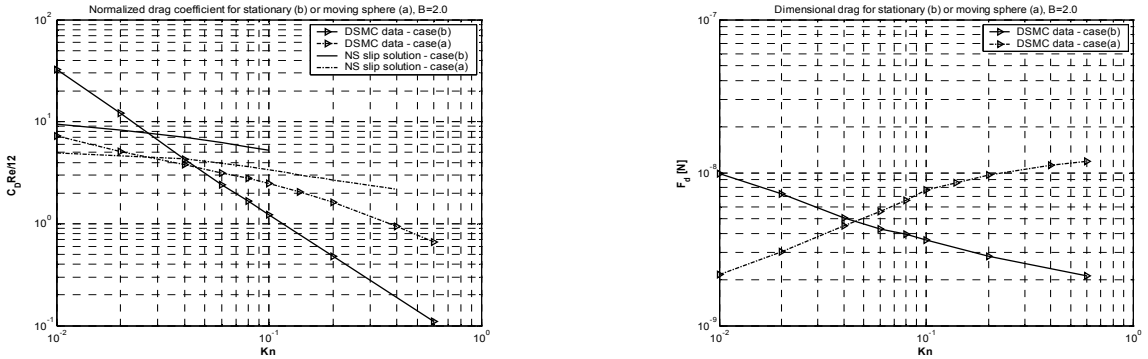

(a) (b)

FIGURE 3. (a) Comparison of normalized drag coefficient versus Knudsen number for the DSMC data (triangles) and the slip-continuum model (lines) for case (a) (dash-dot lines) and case (b) (solid lines); **(b)** Dimensional drag versus *Kn*, for the DSMC data (triangles) for both case (a) and case (b).

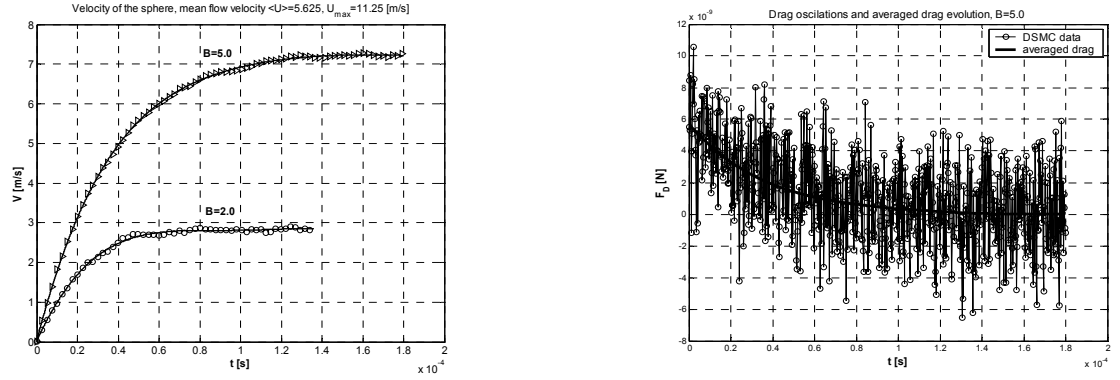

(a) (b)

FIGURE 4. (a) Time evolution of velocity of a confined microsphere dragged by the gas flow. The results are shown for two blockage ratios *B*=2.0 (circles) and *B*=5.0 (triangles); **(b)** Drag oscillations (circles) and filtered mean drag (solid line) for *B*=5.0.

CONCLUSIONS

Slip-continuum and molecular models have been used to compare the drag coefficient on a confined microsphere over a range of Knudsen numbers between 0.01 and 0.4. The results show that the continuum model predicts a larger drag coefficient than the DSMC method when *Kn* is larger than some critical value that depends on the blockage ratio. However, for small *Kn*, the DSMC predictions indicate a larger drag coefficient than the continuum model. This interesting result may be explained by the effects of gas compression in front of the microsphere.

REFERENCES

1. Barber, R. W., and Emerson, D. R., In Rarefied Gas Dynamics: 23rd Int. Symp.-2002, edited by A.D. Ketsdever and E.P. Muntz, AIP Conference Proceedings 663, American Institute of Physics, New York, 2003, pp. 808-815.
2. Ota, M., Kuwahara, K., and Stefanov, S., In Rarefied Gas Dynamics: 23rd Int. Symp.-2002, edited by A.D. Ketsdever and E.P. Muntz, AIP Conference Proceedings 663, American Institute of Physics, New York, 2003, pp. 776-783.
3. Fan, J., and Shen, C., J. Comp. Phys. 167, 393-412 (2001).
4. Beresnev, S. A., Chernyak, V. G., and Fomyagin, G. A., J. Fluid Mechanics 219, 405-421 (1990).
5. Bird, G. A., Molecular Gas Dynamics and the Direct Simulation of Gas Flows, Clarendon Press, Oxford, 1994.
6. Cercignani, C., Pagani, C.D., and Bassanini, P., Phys. Fluids 11, 1399-1403 (1968).
7. Sone, Y., and Aoki, K., "Forces on a Spherical Particle in a Slightly Rarefied Gas", In Rarefied Gas Dynamics: 10th Int. Symp. – 1976, edited by J. Potter, AIAA Progress in Astronautics and Aeronautics 51, New York, 1977, pp. 417-433.